

INFERRING HOST DARK MATTER HALO MASSES OF INDIVIDUAL GALAXIES FROM NEIGHBORING GALAXY COUNTS

MASAMUNE OGURI^{1,2,3} AND YEN-TING LIN^{4,3}

Draft version August 20, 2018

ABSTRACT

How well can we infer host dark matter halo masses of individual galaxies? Based on the halo occupation distribution (HOD) framework, we analytically compute the number of neighboring galaxies within a cylinder of some redshift interval and radius in transverse comoving distance. The result is used to derive the conditional probability distribution function (PDF) of the host halo mass of a galaxy, given the neighboring galaxy counts. We compare our analytic results with those obtained using a realistic mock galaxy catalog, finding reasonable agreements. We find the optimal cylinder radius to be $\sim 0.5 - 1h^{-1}\text{Mpc}$ for the inference of halo masses. The PDF is generally broad, and sometimes has two peaks at low- and high-mass regimes, because of the effect of chance projection along the line-of-sight. Potential applications and extensions of the new theoretical framework developed herein are also discussed.

Keywords: cosmology: theory, cosmology: large-scale structure of Universe, galaxies: formation, galaxies: halos

1. INTRODUCTION

Understanding the connection between galaxies and dark matter halos is one of the most important goals of astrophysics and cosmology. The framework of the halo occupation distribution (HOD) provides a powerful means of studying the relation of galaxy distributions with underlying dark matter distributions (Seljak 2000; Peacock & Smith 2000; Scoccimarro et al. 2001; Cooray & Sheth 2002; Kravtsov et al. 2004; Hamana et al. 2004; Zheng et al. 2005). The HOD characterizes the galaxy bias in terms of the halo occupation number, the average number of galaxies within individual dark halos as a function of halo masses, $\langle N(M) \rangle$, and is very successful in explaining clustering properties of galaxies (e.g., Zehavi et al. 2011; White et al. 2011; Wake et al. 2011; Leauthaud et al. 2012; Coupon et al. 2012; Hikage 2014; More et al. 2014). The idea of the HOD has also been applied to rarer cosmological objects such as quasars (Kayo & Oguri 2012; Richardson et al. 2012; Shen et al. 2013).

The HOD model tells us how galaxies are connected to dark matter halos *statistically*. A natural extension is then to consider how well we can connect galaxies to dark matter halos for *individual* galaxies. Naively we can infer the host halo property of individual galaxies by examining number densities of galaxies around the target galaxies, since a higher number density suggests that the target galaxy is more likely to reside in a group- or cluster-scale dark matter halo. However it is also possible that the galaxy actually resides in a low-mass halo which appears to be associated with a massive halo because of chance projection along the line-of-sight. The redshift information is usually not sufficient to remove

the chance projection, particularly because the observed spatial distributions of galaxies in massive halos are significantly elongated in the redshift direction due to peculiar motions of the galaxies (the so-called Fingers of God effect).

In this paper, we develop a theoretical framework to compute the probability distribution function (PDF) of host halo masses of individual galaxies given number counts of nearby galaxies, assuming that the true HOD is known a priori. We employ the HOD formalism to predict, for each galaxy, the expected number of neighboring galaxies within a cylinder of redshift interval $\pm\Delta z$ and transverse comoving distance within $r_{p,\text{max}}$. We include contributions from both galaxies within the same host halo and those residing in different halos. The result is used to derive the conditional PDF of host halo masses of a galaxy given the neighboring galaxy counts within the cylinder (see also Haas et al. 2012, for a similar study using a semi-analytic model of galaxy formation). We compare our results with those from a mock galaxy catalog constructed from the Millennium Run simulation (Springel et al. 2005; Henriques et al. 2012).

Neighboring galaxy counts, or sometimes referred as counts-in-cylinders, have also been used to constrain the HOD from observations. For instance, Lin, Mohr, & Stanford (2004) directly counted number of galaxies within massive clusters to constrain the HOD at high mass end. Chatterjee et al. (2013) counted the number of quasars in galaxy clusters to try to break degeneracies in the quasar HOD. Reid & Spergel (2009) conducted a counts-in-cylinders analysis to study the HOD of luminous red galaxies (see also Ho et al. 2009). In the previous studies, however, connecting galaxies to dark halos, including the estimate of chance projection, has been attempted rather empirically, e.g., using mock galaxy catalogs. The new theoretical framework developed in this paper provides a more rigorous means of connecting neighboring galaxy counts and the underlying HOD.

The structure of this paper is as follows. In Section 2, we present our analytic model to compute neighboring galaxy counts within the HOD framework. Using the result, in Section 3 we derive conditional PDFs of the host halo mass given neighboring galaxy counts. We compare our analytic model

¹ Research Center for the Early Universe, University of Tokyo, 7-3-1 Hongo, Bunkyo-ku, Tokyo 113-0033, Japan; masamune.oguri@ipmu.jp

² Department of Physics, University of Tokyo, 7-3-1 Hongo, Bunkyo-ku, Tokyo 113-0033, Japan

³ Kavli Institute for the Physics and Mathematics of the Universe (Kavli IPMU, WPI), University of Tokyo, 5-1-5 Kashiwanoha, Kashiwa, Chiba 277-8583, Japan

⁴ Institute of Astronomy and Astrophysics, Academia Sinica, Taipei, Taiwan; ytl@asiaa.sinica.edu.tw

predictions with results from the mock galaxy catalog in Section 4. We discuss possible extensions and applications of our model in Section 5, and give a summary in Section 6. Where necessary we use the Λ -dominated cold dark matter cosmology model employed by the Millennium Run simulation, where $\Omega_m = 0.25$, $\Omega_\Lambda = 0.75$, $H_0 = 100h \text{ km s}^{-1} \text{ Mpc}^{-1}$ with $h = 0.73$, $n_s = 1$, and $\sigma_8 = 0.9$.

2. HALO OCCUPATION DISTRIBUTION APPROACH TO NEIGHBORING GALAXY COUNTS

2.1. Halo occupation distribution

The HOD model specifies the mean halo occupation number $\langle N(M) \rangle$ as a function of halo mass M . Given the mass function and clustering properties of dark matter halos calibrated by N -body simulations, the HOD modeling enables us to analytically compute clustering properties of galaxies. Following Zheng et al. (2005), we consider central and satellite galaxies separately

$$\langle N(M) \rangle = \langle N_{\text{cen}}(M) \rangle + \langle N_{\text{sat}}(M) \rangle, \quad (1)$$

where $\langle N_{\text{cen}}(M) \rangle$ and $\langle N_{\text{sat}}(M) \rangle$ describe the central and satellite components, respectively. We parametrize both components as (e.g., Zheng et al. 2005; White et al. 2011)

$$\langle N_{\text{cen}}(M) \rangle = \frac{1}{2} \text{erfc} \left[\frac{\ln(M_{\text{min}}/M)}{\sqrt{2}\sigma} \right], \quad (2)$$

$$\langle N_{\text{sat}}(M) \rangle = \langle N_{\text{cen}}(M) \rangle \left(\frac{M - \kappa M_{\text{cut}}}{M_1} \right)^\alpha. \quad (3)$$

Here M_{min} is the characteristic minimum mass that can host central galaxies, σ is the characteristic transition width, κM_{cut} is the cutoff mass for satellites, and M_1 and α determine how the mean number of satellite galaxies within halos grows as a function of halo masses (also see Table 1 below). This functional form is motivated by cosmological galaxy formation simulations and is known to explain various observational data very well.

In the following, the galaxies for which we wish to infer host dark matter halo masses are referred to as *target* galaxies, while the galaxies surrounding them (as seen in projection on the sky) are called *neighboring* galaxies. Quantities associated with target (neighboring) galaxies are denoted with a subscript or superscript t (n). The subscript p serves as a reminder when a quantity is evaluated in projection.

2.2. Neighboring galaxy counts

Our primary goal is to compute number counts of neighboring galaxies around a target galaxy. Throughout the paper we count the number of neighboring galaxies within a cylinder defined by a redshift interval $\pm \Delta z$ and transverse comoving distance $r_p < r_{p,\text{max}}$. We denote these neighboring galaxy counts as $N_p = N_p(< r_{p,\text{max}})$. For a galaxy at redshift z , the volume integral of the cylinder is explicitly written as

$$\int dV_c = \int_{z-\Delta z}^{z+\Delta z} \frac{cdz}{H(z)} \int_0^{r_{p,\text{max}}} 2\pi r_p dr_p. \quad (4)$$

It is convenient to derive an explicit expression for the volume integral of the two-point correlation function $\xi(\mathbf{x})$ over the cylinder. Suppose the redshift interval is large enough to include correlated structures, we have

$$\int dV_c \xi(\mathbf{x}) = \int_0^{r_{p,\text{max}}} 2\pi r_p dr_p w_p(r_p). \quad (5)$$

The projected correlation function $w_p(r_p)$ is related to the power spectrum $P(k)$ via

$$w_p(r_p) = \int \frac{k dk}{2\pi} P(k) J_0(kr_p), \quad (6)$$

with $J_\alpha(x)$ being the Bessel functions of the first kind. Using the relation $\int_0^x dx' x' J_0(x') = x J_1(x)$ we then obtain

$$\int dV_c \xi(\mathbf{x}) = \int_0^\infty dk r_{p,\text{max}} P(k) J_1(kr_{p,\text{max}}). \quad (7)$$

2.2.1. 1-halo term

We first consider the so-called 1-halo term, i.e., number counts of neighboring galaxies that reside in the same dark halo. Neighboring galaxy counts should depend on where in the halo the target galaxy is located. We can include this effect by computing neighboring galaxy counts for central and satellite galaxies separately.

Using the expression given in Equation (7), we can derive the average number of neighboring galaxies within the cylinder around a central galaxy as

$$\langle N_p^{\text{1h,c}} \rangle_M = \int_0^\infty dk r_{p,\text{max}} J_1(kr_{p,\text{max}}) \langle N_{\text{sat}}(M) \rangle \tilde{u}(k|M), \quad (8)$$

where $\tilde{u}(k|M)$ is the Fourier transform of the normalized number density profile of satellite galaxies, $u(r|M)$

$$\tilde{u}(k|M) = \int_0^{r_{200c}} 4\pi r^2 dr u(r|M) j_0(kr), \quad (9)$$

with $j_0(x) = \sin(x)/x$ being the spherical Bessel function. In this paper, we define the halo mass M by the total mass within a sphere of r_{200c} , within which the mean density is 200 times the critical density of the Universe. We use this overdensity in order to compare our results with those from the mock galaxy catalog of Henriques et al. (2012, see Section 4). We make the simplifying assumption that the satellite number density profile follows the matter density profile of dark matter (Navarro, Frenk, & White 1997, hereafter NFW)

$$u(r|M) = \frac{\rho(r)}{M} = \frac{\rho_s}{M(r/r_s)(1+r/r_s)^2}, \quad (10)$$

and is truncated at r_{200c} . An important parameter to characterize the NFW profile is concentration $c_{200c} = r_{200c}/r_s$. We use the mass-concentration relation from Duffy et al. (2008)

$$c_{200c} = \frac{5.71}{(1+z)^{0.47}} \left(\frac{M}{2 \times 10^{12} h^{-1} M_\odot} \right)^{-0.084}. \quad (11)$$

Similarly, the 1-halo term of the average number of neighboring galaxies around a satellite galaxy at distance r from the halo center is derived as

$$\langle N_p^{\text{1h,s}(r)} \rangle_M = \int_0^\infty dk r_{p,\text{max}} J_1(kr_{p,\text{max}}) \times [\langle N_{\text{cen}}(M) \rangle + \langle N_{\text{sat}}(M) \rangle \tilde{u}(k|M)] j_0(kr). \quad (12)$$

In each halo with mass M , we can also define the probability of a member galaxy being a central or a satellite galaxy at r as

$$p(c|M) = \frac{\langle N_{\text{cen}}(M) \rangle}{\langle N(M) \rangle}, \quad (13)$$

$$p(s, r|M) = \frac{\langle N_{\text{sat}}(M) \rangle}{\langle N(M) \rangle} u(r|M). \quad (14)$$

The average neighboring galaxy counts within the same halo are then computed as

$$\begin{aligned} \langle N_p^{1h} \rangle_M &= \langle N_p^{1h,c} \rangle_M P(c|M) \\ &+ \int_0^{r_{200c}} 4\pi r^2 dr \langle N_p^{1h,s(r)} \rangle_M P(s,r|M), \\ &= \int_0^\infty dk r_{p,\max} J_1(kr_{p,\max}) \frac{1}{\langle N(M) \rangle} \\ &\times [2\langle N_{\text{cen}}(M) \rangle \langle N_{\text{sat}}(M) \rangle \tilde{u}(k|M) + \langle N_{\text{sat}}(M) \rangle^2 \tilde{u}(k|M)^2]. \end{aligned} \quad (15)$$

On the other hand, the probability distribution of the host dark halo mass is given by

$$p(M) = \frac{1}{\bar{n}} \langle N(M) \rangle \frac{dn}{dM}, \quad (16)$$

where dn/dM is the mass function of dark matter halos, for which we adopt the fitting function of Tinker et al. (2008), and \bar{n} is the average number density of the target/neighboring galaxy population defined by

$$\bar{n} = \int_0^\infty dM \langle N(M) \rangle \frac{dn}{dM}. \quad (17)$$

Hence the average neighboring galaxy counts from galaxies residing in halos of all masses reduce to

$$\begin{aligned} \langle N_p^{1h} \rangle &= \int_0^\infty dM \langle N_p^{1h} \rangle_M P(M) \\ &= \bar{n} \int_0^\infty dk r_{p,\max} P^{1h}(k) J_1(kr_{p,\max}) \\ &= \bar{n} \int dV_c \xi^{1h}(\mathbf{x}), \end{aligned} \quad (18)$$

where $P^{1h}(k)$ is the standard 1-halo term of galaxy power spectrum

$$\begin{aligned} P^{1h}(k) &= \frac{1}{\bar{n}^2} \int_0^\infty dM \frac{dn}{dM} \\ &\times [2\langle N_{\text{cen}}(M) \rangle \langle N_{\text{sat}}(M) \rangle \tilde{u}(k|M) + \langle N_{\text{sat}}(M) \rangle^2 \tilde{u}(k|M)^2]. \end{aligned} \quad (19)$$

2.2.2. 2-halo term and background

Next we consider the 2-halo term, i.e., contributions to neighboring galaxy counts from different halos. We shall include contributions from both the spatially correlated halos and uncorrelated structures along the line-of-sight.

We start by describing neighboring galaxy counts formally as

$$N_p(< r_{p,\max}) = \int dV' n_t(\mathbf{x}') \int dV_c n_n(\mathbf{x} + \mathbf{x}'), \quad (20)$$

where $n_t(\mathbf{x})$ is the number density of the target galaxy. The number density of neighboring galaxies is written using the density fluctuation $\delta_n = \delta_n(\mathbf{x})$ as $n_n(\mathbf{x}) = \bar{n}(1 + \delta_n)$. Since we are interested in a single target galaxy, $n_t(\mathbf{x})$ is written as

$$n_t(\mathbf{x}) = \bar{n}_t(1 + \delta_t) = \delta_D(\mathbf{x} - \mathbf{x}_t), \quad (21)$$

where $\delta_D(\mathbf{x})$ denotes the Dirac delta function, \mathbf{x}_t is the location of that galaxy, and

$$\int dV n_t(\mathbf{x}) = \int dV \bar{n}_t = 1, \quad (22)$$

where the integral is performed over a sufficiently large volume.

The average 2-halo neighboring galaxy counts for the target galaxy in a halo of mass M , including the background contribution, are obtained from Equation (20) as

$$\langle N_p^{2h} \rangle_M = \bar{N}_n + \Delta_{N,\text{tn}}^{2h}. \quad (23)$$

The first term describes the background contribution (or random chance projection), while the second term describes the enhancement of neighboring galaxy counts due to clustering of the underlying matter density field. Each term is explicitly written as

$$\bar{N}_n = \bar{n} \int dV_c, \quad (24)$$

$$\begin{aligned} \Delta_{N,\text{tn}}^{2h} &= \bar{n} \int dV_c \xi_{\text{tn}}^{2h}(\mathbf{x}) \\ &= \bar{n} \int_0^\infty dk r_{p,\max} P_{\text{tn}}^{2h}(k) J_1(kr_{p,\max}). \end{aligned} \quad (25)$$

In practice, there are additional terms originating from higher order correlation functions (see Sec. 39 of Peebles 1980). In this paper we ignore those higher order contributions for simplicity. As we will see below, this is a reasonably good approximation in our case where we study number counts projected over redshift ranges that is much larger than typical correlating lengths ($\mathcal{O}(10)$ Mpc). The 2-halo term of the power spectrum is simply given by

$$P_{\text{tn}}^{2h}(k) = b(M) \bar{b} P_m(k), \quad (26)$$

where $b(M)$ is the halo bias for which we adopt a fitting function of Tinker et al. (2010), $P_m(k)$ is the linear matter power spectrum (computed using the fitting formulae of Eisenstein & Hu 1999), and \bar{b} is the average galaxy bias computed by

$$\bar{b} = \frac{1}{\bar{n}} \int_0^\infty dM b(M) \langle N(M) \rangle \frac{dn}{dM}. \quad (27)$$

Again by averaging $\langle N_p^{2h} \rangle_M$ over $p(M)$ (Equation 16) we deduce an expression similar to Equation (18)

$$\begin{aligned} \langle N_p^{2h} \rangle &= \int_0^\infty dM \langle N_p^{2h} \rangle_M P(M) \\ &= \bar{N}_n + \bar{n} \int dV_c \xi^{2h}(\mathbf{x}), \end{aligned} \quad (28)$$

where $\xi^{2h}(\mathbf{x})$ is the Fourier transform of the two-halo galaxy power spectrum $P^{2h}(k) = \bar{b}^2 P_m(k)$.

Based on this formalism we can also derive the variance of neighboring galaxy counts in the limit of $\int dV \rightarrow \infty$ as

$$(\sigma_p^{2h})^2 \equiv \langle N_p^{2h} N_p^{2h} \rangle_M - \langle N_p^{2h} \rangle_M^2 = \bar{N}_n + \bar{N}_n \Delta_{N,\text{nn}}^{2h}, \quad (29)$$

where

$$\begin{aligned} \Delta_{N,\text{nn}}^{2h} &= \frac{\bar{n}^2}{\bar{N}_n} \int dV_c \int dV_c' \xi_{\text{nn}}^{2h}(\mathbf{x} - \mathbf{x}') \\ &= \bar{n} \int_0^\infty \frac{2dk}{k} P_{\text{nn}}^{2h}(k) [J_1(kr_{p,\max})]^2, \end{aligned} \quad (30)$$

with $P_{\text{nn}}^{2h}(k) = P^{2h}(k) = \bar{b}^2 P_m(k)$. Again, we have ignored contributions from higher order correlations.

3. PROBABILITY DISTRIBUTIONS OF NEIGHBORING GALAXY COUNTS AND HOST DARK HALO MASSES

3.1. Probability distribution of neighboring galaxy counts

We start by deriving the PDF of neighboring galaxy counts around a target galaxy that resides in a dark halo with mass M . For this purpose, we adopt the following assumptions: (1) the PDF of 1-halo neighboring galaxy counts follows the Poisson distribution, which is a reasonable assumption at least for massive halos where $\langle N(M) \rangle$ is large (e.g., Lin, Mohr, & Stanford 2004; Zheng et al. 2005), (2) the PDF of 2-halo plus background neighboring galaxy counts follows the log-normal distribution, given that the probability distribution function of cosmological density fields is accurately described by the log-normal distribution (e.g., Kayo, Taruya, & Suto 2001), and (3) the 1-halo and 2-halo PDFs are uncorrelated with each other.

For the expected value of λ , the Poisson distribution gives the PDF of observed number N as

$$p^P(N|\lambda) = \frac{\lambda^N e^{-\lambda}}{N!}. \quad (31)$$

We include the position dependence of the galaxy in the calculation of the PDF of 1-halo neighboring galaxy counts. Using the results given in Section 2.2.1, we obtain

$$p^{1h}(N_p^{1h}|M) = p^P(N_p^{1h}|\langle N_p^{1h,c} \rangle_M) p(c|M) + \int_0^{r_{200c}} 4\pi r^2 dr p^P(N_p^{1h}|\langle N_p^{s(r)} \rangle_M) p(s, r|M). \quad (32)$$

We assume that the PDF of 2-halo neighboring galaxy counts follows the log-normal distribution

$$p^{LN}(N|\mu, s) = \frac{1}{N\sqrt{2\pi}s} e^{-\frac{(\ln N - \mu)^2}{2s^2}}. \quad (33)$$

Detailed discussions on the validity of this assumption are given in Appendix. We then obtain

$$p^{2h}(N_p^{2h}|M) = p^{LN}(N_p^{2h}|\mu_M, s_M), \quad (34)$$

where the parameters μ_M and s_M are related to the mean $\langle N_p^{2h} \rangle$ and variance $(\sigma_p^{2h})^2$ as

$$\mu_M = \ln \frac{\langle N_p^{2h} \rangle^2}{\sqrt{\langle N_p^{2h} \rangle^2 + (\sigma_p^{2h})^2}}, \quad (35)$$

$$s_M^2 = \ln \left[1 + \frac{(\sigma_p^{2h})^2}{\langle N_p^{2h} \rangle^2} \right]. \quad (36)$$

Finally we combine these two PDFs to obtain the PDF of total neighboring galaxy counts

$$p(N_p|M) = \sum_{N=0}^{N_p} p^{1h}(N_p - N|M) p^{2h}(N|M). \quad (37)$$

3.2. Probability distribution of host halo masses

We now turn the problem around and ask how well we can infer the host halo mass of a single target galaxy from observed neighboring galaxy counts. This is obtained by using the Bayes' theorem

$$p(M|N_p) = \frac{p(N_p|M)p(M)}{\int dM p(N_p|M)p(M)}, \quad (38)$$

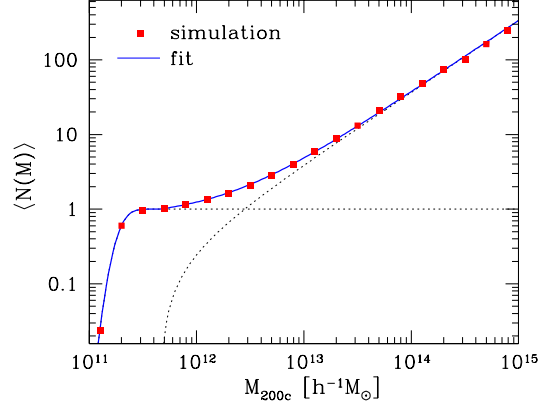


Figure 1. The mean halo occupation number of the mock galaxy catalog. Filled squares show the mean occupation number directly obtained from the mock catalog. The solid line is best-fitting halo occupation number with Equations (2) and (3). Dotted curves represent contributions from the central and satellite components. Best-fit parameters are summarized in Table 1.

Table 1
Best-fit HOD parameters

Parameter	Best-fit value
$M_{\min}[h^{-1}M_{\odot}]$	$10^{11.277}$
σ	0.207
$\kappa M_{\text{cut}}[h^{-1}M_{\odot}]$	$10^{11.666}$
$M_1[h^{-1}M_{\odot}]$	$10^{12.370}$
α	0.960

where $p(N_p|M)$ and $p(M)$ are given in Equations (37) and (16), respectively.

4. COMPARISON WITH THE MOCK GALAXY CATALOG

4.1. Mock galaxy catalog

We use the all-sky light-cone mock catalog from Henriques et al. (2012) to test our analytic predictions. This mock is based on the semi-analytic model of Guo et al. (2011), and is constructed by replicating the Millennium Run simulation box ($500h^{-1}\text{Mpc}$ on a side) without transformations such as rotation, translation, or inversion. Guo et al. (2011) showed that their model can reproduce important statistical properties of nearby galaxies such as the stellar mass function and two-point correlation function.

For each galaxy in the mock, information such as the sky position, redshift, apparent and absolute magnitudes, host dark matter halo mass, and central/satellite designation, is available. The catalog is flux limited to $i < 21$. In this paper, we generate a volume-limited galaxy subsample of $M_i < -20$ to about $z = 0.2$ and use the subsample for our analysis.

4.2. Halo occupation number

An essential ingredient in our formalism is the halo occupation number $\langle N(M) \rangle$. In the mock galaxy catalog, we know host halo properties of individual galaxies, which allows us to derive the mean halo occupation number directly without ambiguity. We fit the halo occupation number obtained directly from the mock catalog to the parametrized form in Equations (2) and (3), which contains five free parameters in total. We show the fitting result in Figure 1, and summarize best-fit parameters in Table 1. We find that the HOD model adopted in this paper reproduces the mean occupation number in the mock galaxy catalog very well.

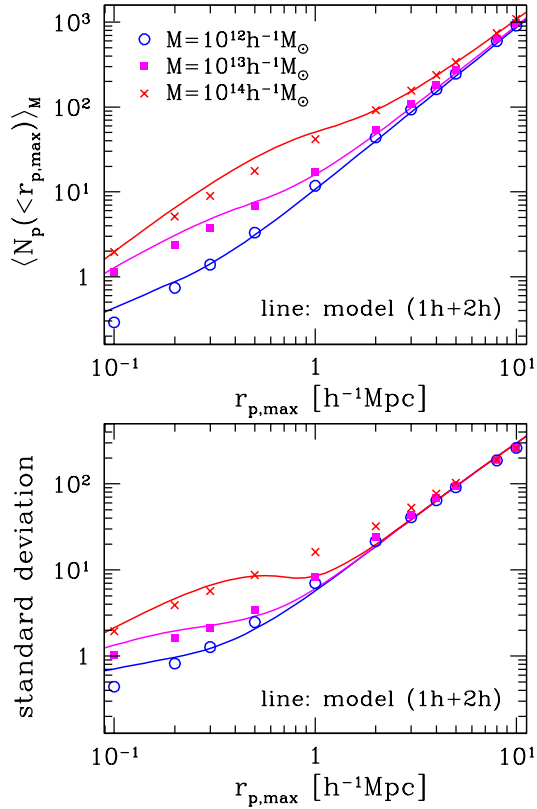


Figure 2. The average neighboring galaxy counts within the comoving transverse distance $r_{p,\max}$. The number counts are computed around galaxies at $z = 0.15$ which reside in host halos with mass M . The redshift range of the neighboring galaxies is set to $z = 0.15 \pm 0.02$. Symbols show the result from the mock galaxy catalog for host halo masses of $M = 10^{12}$ (open circles), 10^{13} (filled squares), and $10^{14} h^{-1} M_\odot$ (crosses), and solid lines show corresponding analytic model predictions including both 1-halo and 2-halo contributions. The upper panel shows the average neighboring galaxy counts $\langle N_p(<r_{p,\max}) \rangle_M$ (Equation 39), whereas the lower panel shows its standard deviation σ_p (Equation 40).

4.3. Neighboring galaxy counts

Before comparing the PDF of the halo mass, we first check whether our analytic model reproduces neighboring galaxy counts in the mock galaxy catalog. The average (projected) neighboring galaxy counts around a galaxy inside a halo with mass M is given by

$$\langle N_p(<r_{p,\max}) \rangle_M = \langle N_p^{1h} \rangle_M + \langle N_p^{2h} \rangle_M, \quad (39)$$

where $\langle N_p^{1h} \rangle_M$ and $\langle N_p^{2h} \rangle_M$ are given in Equations (15) and (28), respectively.

We compute neighboring galaxy counts as a function of the maximum comoving transverse distance $r_{p,\max}$. The redshift of target galaxies for which neighboring galaxy counts are considered is arbitrarily fixed at $z = 0.15$. In the mock galaxy catalog, we actually use galaxies in the small redshift range of $z = 0.15 \pm 0.005$. Throughout the paper we consider the redshift range of neighboring galaxies of $\Delta z = 0.02$, which is sufficiently large to include the correlated structure.

Figure 2 (upper panel) compares the average neighboring galaxy counts from the mock galaxy catalog with the analytic calculation (Equation 39). We consider target galaxies living in halos of three masses, $M = 10^{12}$, 10^{13} , and $10^{14} h^{-1} M_\odot$, and find that our model agrees well with the mock result, both at small and large $r_{p,\max}$ where 1-halo and 2-halo contributions are dominated, respectively. As expected, neighboring galaxy

counts are higher for galaxies in more massive host halos.

We also check the variance of the average neighboring galaxy counts, $\sigma_p^2 \equiv \langle N_p N_p \rangle_M - \langle N_p \rangle_M^2$. Again, the variance is given by the sum of 1-halo and 2-halo contributions

$$\sigma_p^2 = (\sigma_p^{1h})^2 + (\sigma_p^{2h})^2, \quad (40)$$

where $(\sigma_p^{2h})^2$ is derived in Equation (29). Given the PDF of 1-halo neighboring galaxy counts (Equation 32), we can compute $(\sigma_p^{1h})^2$ as

$$\begin{aligned} (\sigma_p^{1h})^2 = & \langle N_p^{1h} \rangle_M - \langle N_p^{1h} \rangle_M^2 + \langle N_p^{1h,c} \rangle_M^2 p(c|M) \\ & + \int_0^{r_{200c}} 4\pi r^2 dr \langle N_p^{1h,s(r)} \rangle_M^2 p(s,r|M). \end{aligned} \quad (41)$$

The comparison shown in Figure 2 (lower panel) indicates that the analytic model reproduces the variance as well, in both 1-halo and 2-halo regimes. However there is relatively large deviation of the analytic model at $r_{p,\max} \sim 1 h^{-1} \text{Mpc}$ for the host halo mass of $M = 10^{14} h^{-1} M_\odot$. This might be explained by the non-Gaussian error of the 2-halo term at very small scale. Another possible explanation of the discrepancy is the presence of satellite galaxies outside r_{200c} ; we find that the mock galaxy catalog contains satellite galaxies that are located outside r_{200c} ($\sim 10\%$), whereas we have assumed that all satellite galaxies are located within r_{200c} .

4.4. PDF of host halo masses

We now compare our model of PDFs of the host halo masses given neighboring galaxy counts, $p(M|N_p)$ (Equation 38), with those obtained directly from the mock galaxy catalog. Figure 3 compares the PDFs from the mock galaxy catalog with our analytic model. We find that our analytic models are in reasonably good agreement with the simulation result. In particular the analytic model nicely captures the complex behaviors of the PDFs.

We find the PDF exhibits two peaks when the number of neighboring galaxies N_p is large. The higher mass peak corresponds to the case that the galaxy resides in massive halos with about the peak mass. On the other hand, the lower mass peak is due to the chance projection, i.e., the low-mass host halo of the galaxy is superposed on a massive halo or a dense structure on the sky, which boosts the neighboring galaxy counts. Our analytic model reproduces this behavior.

We find that the dependence of the PDFs on neighboring galaxy counts is weak for the large cylinder radius of $r_{p,\max} = 8 h^{-1} \text{Mpc}$ for which the contribution is dominated by the 2-halo term. Although neighboring galaxy counts depend on the host halo mass due to the halo mass dependence of the halo bias, neighboring galaxy counts also involves the large scatter originating from clustering of neighboring galaxies (see Figure 2). Thus, in order to infer the host halo mass of individual galaxies, small cylinder radii of $r_{p,\max} \lesssim 1 h^{-1} \text{Mpc}$ should be used for neighboring galaxy counts.

With the analytic model of PDFs of the host halo masses, we can easily explore how different choices of neighboring counts provide tighter constraints on halo masses. In addition to $r_{p,\max}$ discussed above, we can also adjust the redshift range Δz . Here we demonstrate how we can optimize $r_{p,\max}$ and Δz from the PDFs. As a specific example, we consider an input halo mass of $M = 10^{14} h^{-1} M_\odot$. We first compute the average neighboring number $\langle N_p(<r_{p,\max}) \rangle_M$ (Equation 39) for given values of $r_{p,\max}$ and Δz , and compute the conditional PDF

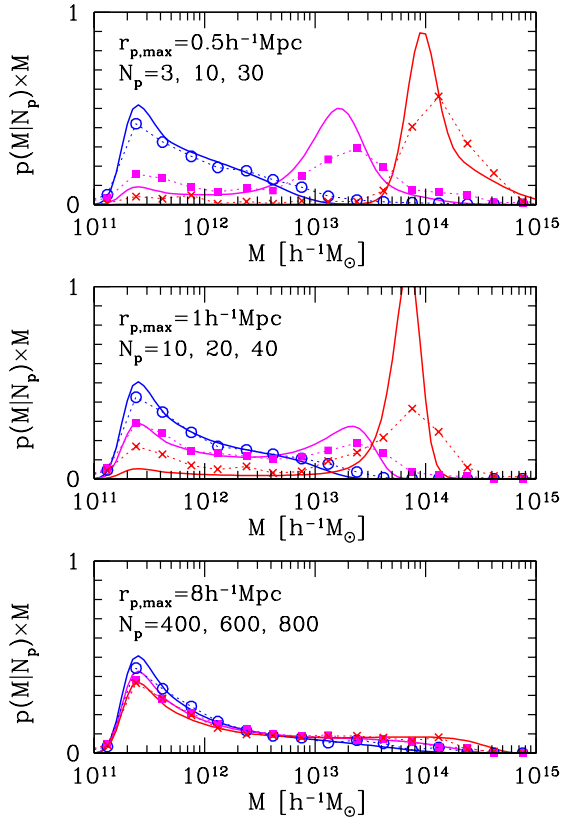


Figure 3. PDFs of the host halo masses of galaxies with neighboring galaxy counts within $r_{p,\max}$ being N_p , $p(M|N_p)$. From top to bottom panels, we consider three different maximum comoving transverse distance, $r_{p,\max} = 0.5, 1,$ and $8h^{-1}\text{Mpc}$, within which the number of neighboring galaxy is counted. Different symbols show conditional PDFs for different neighboring galaxy counts N_p from the mock galaxy catalog, and corresponding analytic model predictions (Equation 38) are plotted by solid lines.

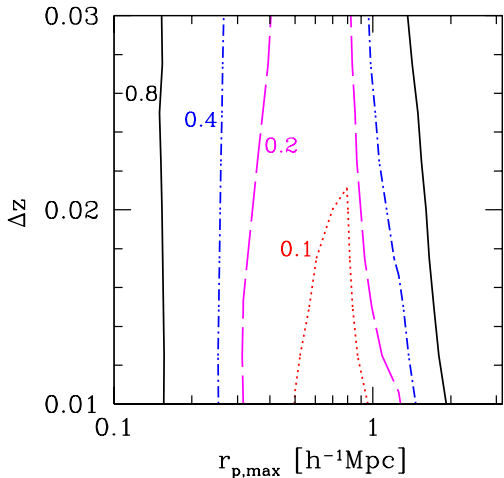


Figure 4. Contours of the variance of inferred host halo masses, $\sigma_{\log M}^2$ which is computed from the conditional PDF $p(M|N_p)$, in the $r_{p,\max}-\Delta z$ plane. The input halo mass is $M = 10^{14}h^{-1}M_\odot$, and the average neighboring number $\langle N_p(< r_{p,\max}) \rangle_M$ (Equation 39) is used for the input N_p to compute the PDF. Dotted, dashed, dot-dashed, and solid lines show contours of $\sigma_{\log M}^2 = 0.1, 0.2, 0.4,$ and 0.8 , respectively.

$p(M|N_p)$ (Equation 38) given the number count N_p equal to the average neighboring number. We quantify the tightness of the halo mass inference by computing the variance of the halo mass $\log M$, $\sigma_{\log M}^2$, using the computed PDF. Smaller $\sigma_{\log M}^2$ indicates a narrower peak of the PDF and therefore tighter constraints on the halo mass. The contours shown in Figure 4 confirm that cylinder radii of $r_{p,\max} \sim 0.5-1h^{-1}\text{Mpc}$ provide tightest constraints on the halo masses. We find that the dependence on Δz is not very strong, but smaller Δz generally produces tighter constraints, because of the smaller number of projected galaxies. We note that the best choice of the parameters depends also on other factors such as halo masses and underlying HOD models.

5. EXTENSIONS AND APPLICATIONS

In Section 4 we have used a mock galaxy catalog to demonstrate that our analytic model can robustly predict the PDF of halo mass for a *single* galaxy, given its neighboring counts. Although the example we have considered is somewhat idealized (i.e., with 100% spectroscopic sampling and redshift success rate), we note that these conditions are not required. In principle, for a given galaxy sample, as long as we can accurately model its HOD, our model can be used to predict the host halo mass PDF for the galaxies *in* the sample.

Here we briefly discuss various ways to extend the scope and capabilities of our model, including the possibility to distinguish central galaxies from satellites, the situation when the target and neighboring galaxies are from two different galaxy samples, the potential of improving the PDF with neighboring counts within multiple apertures, constraints on the HOD itself, the application to galaxy samples selected with photometric redshifts, and the prospect of applying the same principle to inferring masses of galaxy clusters.

5.1. Probability of being central

In many of HOD studies, central and satellite components are treated separately. Therefore it is of great interest to know whether each galaxy corresponds to the central or satellite type. This can be obtained easily in this theoretical framework. From Equation (32), we derive the joint probability of being a central galaxy and having a 1-halo neighboring galaxy count of N_p^{1h} as

$$p^{\text{1h}}(c, N_p^{\text{1h}}|M) = p^{\text{P}}(N_p^{\text{1h}}|\langle N_p^{\text{1h},c} \rangle_M)p(c|M), \quad (42)$$

By replacing $p^{\text{1h}}(N_p - N|M)$ in Equation (37) with $p^{\text{1h}}(c, N_p - N|M)$ and inserting the result to Equation (38), we obtain the joint PDF of $p(c, M|N_p)$. The probability of being central given the host halo mass M and neighboring galaxy count N_p is then obtained as

$$p(c|M, N_p) = \frac{p(c, M|N_p)}{p(M|N_p)}. \quad (43)$$

Figure 5 shows some examples of $p(c|M, N_p)$ for the cylinder of radius $r_{p,\max} = 0.5h^{-1}\text{Mpc}$. The probability is generally higher for smaller halo masses, simply because there are fewer satellite galaxies in lower mass halos (see Figure 1). On the other hand, the probabilities shown in Figure 5 exhibit dependences on neighboring galaxy counts N_p , suggesting that neighboring galaxy counts do provide information when determining whether a galaxy is central or not.

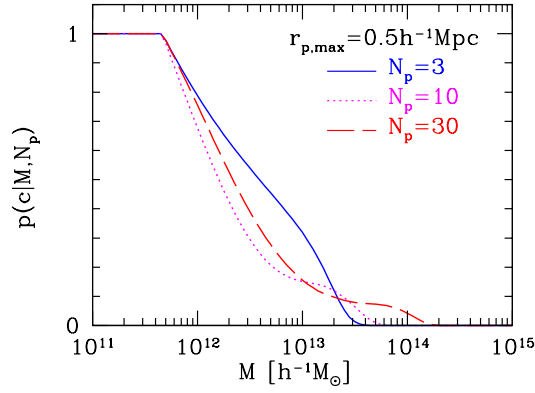


Figure 5. The probability of being a central galaxy given the halo mass and neighboring galaxy counts (Equation 43). The cylinder radius is fixed to $r_{p,\max} = 0.5h^{-1}\text{Mpc}$. We consider three different N_p : $N_p = 3$ (solid), 10 (dotted), and 30 (dashed).

5.2. The use of different galaxy populations

While we have assumed that the target galaxy for which we infer the host halo mass and neighboring galaxies are the same population and they share the same HOD, in principle we can use populations with different HODs for neighboring galaxy counts (e.g., red and blue galaxies, galaxies of different luminosity/stellar mass, or groups/clusters instead of galaxies). The extension of our theoretical framework to this situation is straightforward. Suppose the halo occupation number of the target galaxy $\langle N^t(M) \rangle$ differs from that of neighboring galaxies $\langle N^n(M) \rangle$, the 1-halo neighboring galaxy counts are modified as

$$\langle N_p^{\text{1h,c}} \rangle_M = \int_0^\infty dk r_{p,\max} J_1(kr_{p,\max}) \langle N_{\text{sat}}^n(M) \rangle \tilde{u}_n(k|M), \quad (44)$$

$$\langle N_p^{\text{1h,s}(r)} \rangle_M = \int_0^\infty dk r_{p,\max} J_1(kr_{p,\max}) \times [\langle N_{\text{cen}}^t(M) \rangle + \langle N_{\text{sat}}^n(M) \rangle \tilde{u}_n(k|M)] j_0(kr), \quad (45)$$

$$p(c|M) = \frac{\langle N_{\text{cen}}^t(M) \rangle}{\langle N^t(M) \rangle}, \quad (46)$$

$$p(s, r|M) = \frac{\langle N_{\text{sat}}^n(M) \rangle}{\langle N^t(M) \rangle} u_t(r|M), \quad (47)$$

where u_t and u_n are spatial distributions of satellite components of target and neighboring galaxies, respectively, and the PDF of the host halo mass becomes

$$p(M) = \frac{1}{\bar{n}_t} \langle N^t(M) \rangle \frac{dn}{dM}, \quad (48)$$

and the average bias for the 2-halo calculation becomes

$$\bar{b}_n = \frac{1}{\bar{n}_n} \int_0^\infty dM b(M) \langle N^n(M) \rangle \frac{dn}{dM}, \quad (49)$$

where \bar{n}_t and \bar{n}_n are average number densities (see Equation 17) of target and neighboring galaxies, respectively. Also note that \bar{n} in $\langle N_p^{\text{2h,c}} \rangle_M$ should be interpreted as \bar{n}_n . Since different galaxy populations probe different halo masses, the use of different galaxy populations for neighboring galaxy counts can help improve the inference of the host halo mass.

5.3. The use of multiple apertures

The inference of the host halo mass may be improved further by considering multiple apertures, i.e., combining neighboring galaxy counts with different cylinder radii. In this case, we need to take account of the covariance of neighboring galaxy counts carefully. We leave the exploration of this possibility for future work.

5.4. Improving the analytic model

There is also room for the improvement of our analytic model. For instance, attempts to improve the halo model have been made by including the halo exclusion effect and non-linearity of the 2-halo power spectrum (e.g., Tinker et al. 2005). The evaluation of non-Gaussian error may be necessary to improve the estimate of the variance of 2-halo neighboring galaxy counts, $(\sigma_p^{\text{2h}})^2$ (see Figure 2). We have also ignored the complexity of the halo properties, such as the scatter in the concentration parameter and the halo triaxiality. The HOD model itself is also subject to possible improvements, e.g., by including assembly bias (Wang et al. 2013; Zentner et al. 2014; Lacerna et al. 2014) and relative velocities of central galaxies (Skibba et al. 2011).

5.5. Constraints on HOD with counts-in-cylinders

Neighboring galaxy counts depend on the underlying HOD model, and therefore in principle they can be used to constrain the HOD itself. For this application, it is crucial to estimate and remove the chance projection. One can infer the effect of pure chance projection by estimating the average number density, but the 2-halo contribution is not homogeneous but clustered around the target galaxy. The theoretical framework developed in this paper may be used to estimate the 2-halo contribution and its variance to derive more rigorous constraints on HOD with counts-in-cylinders.

5.6. Extension to galaxy samples with photometric redshifts

Although our formalism is readily applicable to several spectroscopic surveys such as Sloan Digital Sky Survey (SDSS; York et al. 2000), Galaxy And Mass Assembly (GAMA; Driver et al. 2011), PRISM Multi-object Survey (PRIMUS; Coil et al. 2011), VIMOS Public Extragalactic Redshift Survey (VIPERS; Guzzo et al. 2014), and eventually Dark Energy Spectroscopic Instrument (DESI; Levi et al. 2013), and Subaru Prime Focus Spectrograph (PFS; Takada et al. 2014), it is highly desirable to extend our model to incorporate samples selected with photometric redshifts, so that we could fully exploit the potential offered by large imaging surveys such as Subaru Hyper Suprime-Cam (HSC; Miyazaki et al. 2012) survey, Dark Energy Survey⁵, and Large Synoptic Survey Telescope (LSST; LSST Science Collaboration et al. 2009). We plan to address this extension in a future paper.

5.7. Inferring galaxy cluster masses using neighboring cluster counts

Galaxy clusters have long been regarded as a powerful cosmological probe, as their abundance is sensitively dependent on parameters such as Ω_m and σ_8 . Accurate knowledge of cluster mass is required, however, before any useful cosmological constraints can be deduced (Weinberg et al. 2013).

⁵ <http://www.darkenergysurvey.org/>

Our formalism could be straightforwardly applied to galaxy clusters, especially samples detected in optical/near-IR imaging surveys, for which it has typically been difficult to deduce mass reliably for individual clusters. With the knowledge of PDF of cluster mass, it should be possible to obtain tighter constraints from cluster abundance.

6. SUMMARY

In the highly successful HOD framework, the dark matter halo mass is the sole factor controlling the galaxy formation process. It is thus critically important to be able to estimate the halo mass of galaxies. Traditionally, this is achieved by techniques such as strong gravitational lensing (e.g., Bolton et al. 2008), galaxy-galaxy lensing (e.g., Mandelbaum et al. 2006), satellite kinematics (e.g., More et al. 2009), and large scale clustering (e.g., Zehavi et al. 2011). Except for the first method, all the others work in a statistical sense, that is, they cannot be applied to a single galaxy. An alternative method is developed by Yang et al. (2005), where the concept of abundance matching is employed to a large group catalog which includes groups with only one member. Under the assumption of one-to-one correspondence between halo mass and stellar mass/luminosity content of the group members, a halo mass is *assigned* to each of the groups. However, with this approach, little or no information on the PDF of the halo mass is provided. Furthermore, given the difficulties in constructing group catalog at low mass halo regime and the associated uncertainties, the one-to-one correspondence between these groups and dark halos is likely to break down, rendering halo mass assignment unreliable.

We have developed a theoretical framework to compute the PDF of the host halo mass for a single galaxy, given its neighboring galaxy counts. We have derived explicit expression for the number of neighboring galaxies within the cylinder of redshift interval $\pm\Delta z$ and transverse comoving distance $r_p < r_{p,\max}$ in terms of the HOD model. We include both 1-halo contribution from the same host halo and 2-halo contribution including chance projection for the neighboring galaxy counts. We have used the result to obtain the conditional PDF of the host halo mass given neighboring galaxy counts.

We compare our analytic model with results from the mock galaxy catalog, finding reasonable agreements. The PDF of the host halo mass exhibits complex behavior, with generally two peaks at low- and high-mass regimes for the case of large neighboring galaxy counts. This is understood as the effect of chance projection along the line-of-sight, which can boost neighboring galaxy counts even if the host halo is a low-mass halo. We find that cylinder radii of $\sim 0.5 - 1h^{-1}\text{Mpc}$ are optimal for the inference of the host halo mass, at least for the case of the HOD examined in this paper.

This paper serves as a proof-of-concept for our theoretical framework, and we expect our new approach to have many applications.

ACKNOWLEDGMENTS

We thank an anonymous referee for useful comments and suggestions. This work was supported in part by World Premier International Research Center Initiative (WPI Initiative), MEXT, Japan, and Grant-in-Aid for Scientific Research from the JSPS (26800093). MO acknowledges the hospitality of ASIAA where this work was partly done. YTL acknowledges support from the Ministry of Science and Technology grant

NSC 102-2112-M-001-001-MY3 and the hospitality of Kavli IPMU where this work was initiated.

REFERENCES

- Bolton, A. S., Burles, S., Koopmans, L. V. E., et al. 2008, *ApJ*, 682, 964
 Chatterjee, S., Nguyen, M. L., Myers, A. D., & Zheng, Z. 2013, *ApJ*, 779, 147
 Coil, A. L., Blanton, M. R., Burles, S. M., et al. 2011, *ApJ*, 741, 8
 Cooray, A., & Sheth, R. 2002, *Phys. Rep.*, 372, 1
 Coupon, J., Kilbinger, M., McCracken, H. J., et al. 2012, *A&A*, 542, A5
 Driver, S. P., Hill, D. T., Kelvin, L. S., et al. 2011, *MNRAS*, 413, 971
 Duffy, A. R., Schaye, J., Kay, S. T., & Dalla Vecchia, C. 2008, *MNRAS*, 390, L64
 Eisenstein, D. J., & Hu, W. 1999, *ApJ*, 511, 5
 Guo, Q., White, S., Boylan-Kolchin, M., et al. 2011, *MNRAS*, 413, 101
 Guzzo, L., Scodreggio, M., Garilli, B., et al. 2014, *A&A*, 566, A108
 Haas, M. R., Schaye, J., & Jeesson-Daniel, A. 2012, *MNRAS*, 419, 2133
 Hamana, T., Ouchi, M., Shimasaku, K., Kayo, I., & Suto, Y. 2004, *MNRAS*, 347, 813
 Henriques, B. M. B., White, S. D. M., Lemson, G., et al. 2012, *MNRAS*, 421, 2904
 Hikage, C. 2014, *MNRAS*, 441, L21
 Ho, S., Lin, Y.-T., Spergel, D., & Hirata, C. M. 2009, *ApJ*, 697, 1358
 Kayo, I., & Oguri, M. 2012, *MNRAS*, 424, 1363
 Kayo, I., Taruya, A., & Suto, Y. 2001, *ApJ*, 561, 22
 Kravtsov, A. V., Berlind, A. A., Wechsler, R. H., Klypin, A. A., Gottlöber, S., Allgood, B., & Primack, J. R. 2004, *ApJ*, 609, 35
 Lacerna, I., Padilla, N., & Staszyszyn, F. 2014, *MNRAS*, 443, 3107
 Leauthaud, A., Tinker, J., Bundy, K., et al. 2012, *ApJ*, 744, 159
 Levi, M., Bebek, C., Beers, T., et al. 2013, *arXiv:1308.0847*
 Lin, Y.-T., Mohr, J. J., & Stanford, S. A. 2004, *ApJ*, 610, 745
 LSST Science Collaboration, Abell, P. A., Allison, J., et al. 2009, *arXiv:0912.0201*
 Mandelbaum, R., Seljak, U., Kauffmann, G., Hirata, C. M., & Brinkmann, J. 2006, *MNRAS*, 368, 715
 Miyazaki, S., Komiyama, Y., Nakaya, H., et al. 2012, *Proc. SPIE*, 8446, 84460Z
 More, S., van den Bosch, F. C., Cacciato, M., et al. 2009, *MNRAS*, 392, 801
 More, S., Miyatake, H., Mandelbaum, R., Takada, M., Spergel, D., Brownstein, J., & Schneider, D. P. 2014, *arXiv:1407.1856*
 Navarro, J. F., Frenk, C. S., & White, S. D. M. 1997, *ApJ*, 490, 493
 Peacock, J. A., & Smith, R. E. 2000, *MNRAS*, 318, 1144
 Peebles, P. J. E. 1980, *The Large-scale Structure of the Universe* (Princeton, NJ: Princeton Univ. Press)
 Reid, B. A., & Spergel, D. N. 2009, *ApJ*, 698, 143
 Richardson, J., Zheng, Z., Chatterjee, S., Nagai, D., & Shen, Y. 2012, *ApJ*, 755, 30
 Scoccimarro, R., Sheth, R. K., Hui, L., & Jain, B. 2001, *ApJ*, 546, 20
 Seljak, U. 2000, *MNRAS*, 318, 203
 Shen, Y., McBride, C. K., White, M., et al. 2013, *ApJ*, 778, 98
 Skibba, R. A., van den Bosch, F. C., Yang, X., et al. 2011, *MNRAS*, 410, 417
 Springel, V., White, S. D. M., Jenkins, A., et al. 2005, *Nature*, 435, 629
 Takada, M., Ellis, R. S., Chiba, M., et al. 2014, *PASJ*, 66, 1
 Tinker, J. L., Weinberg, D. H., Zheng, Z., & Zehavi, I. 2005, *ApJ*, 631, 41
 Tinker, J., Kravtsov, A. V., Klypin, A., Abazajian, K., Warren, M., Yepes, G., Gottlöber, S., & Holz, D. E. 2008, *ApJ*, 688, 709
 Tinker, J. L., Robertson, B. E., Kravtsov, A. V., Klypin, A., Warren, M. S., Yepes, G., & Gottlöber, S. 2010, *ApJ*, 724, 878
 Wake, D. A., Whitaker, K. E., Labbé, I., et al. 2011, *ApJ*, 728, 46
 Wang, L., Weinmann, S. M., De Lucia, G., & Yang, X. 2013, *MNRAS*, 433, 515
 Weinberg, D. H., Mortonson, M. J., Eisenstein, D. J., et al. 2013, *Phys. Rep.*, 530, 87
 White, M., Blanton, M., Bolton, A., et al. 2011, *ApJ*, 728, 126
 Yang, X., Mo, H. J., van den Bosch, F. C., & Jing, Y. P. 2005, *MNRAS*, 356, 1293
 York, D. G., Adelman, J., Anderson, J. E., Jr., et al. 2000, *AJ*, 120, 1579
 Zehavi, I., Zheng, Z., Weinberg, D. H., et al. 2011, *ApJ*, 736, 59
 Zentner, A. R., Hearin, A. P., & van den Bosch, F. C. 2014, *MNRAS*, 443, 3044
 Zheng, Z., Berlind, A. A., Weinberg, D. H., et al. 2005, *ApJ*, 633, 791

VALIDITY OF THE LOG-NORMAL ASSUMPTION FOR THE PDF OF 2-HALO NEIGHBORING GALAXY COUNTS

We assumed that the PDF of 2-halo neighboring galaxy counts follows the log-normal distribution (Equation 33)

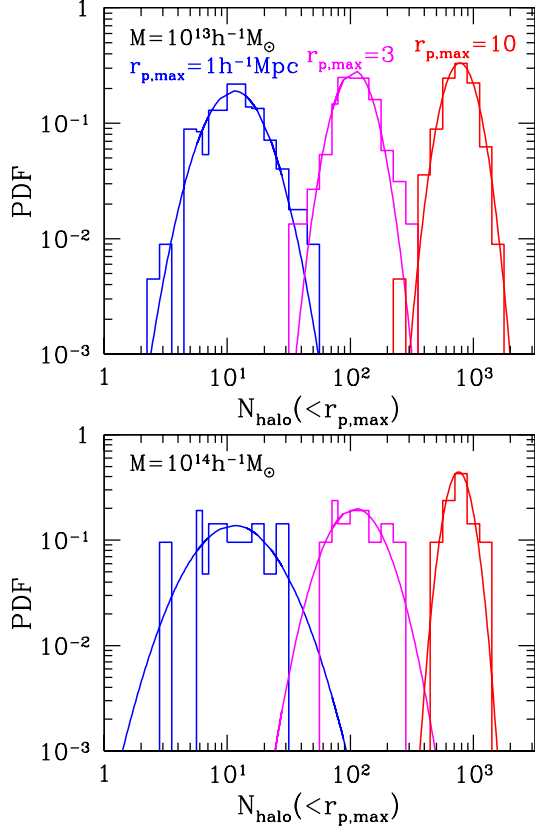


Figure A1. The PDFs of number counts of dark matter halos ($M \geq 10^{11} h^{-1} M_{\odot}$) around halos with masses $M = 10^{13} h^{-1} M_{\odot}$ (upper panel) and $10^{14} h^{-1} M_{\odot}$ (lower panel). In each panel, we plot the PDFs for three different maximum transverse separations, $r_{p,\max} = 1, 3,$ and $10 h^{-1} \text{Mpc}$. Histograms show PDFs measured directly in the Millennium Run simulation (see Section 4 for details), whereas solid lines show best-fit log-normal distributions.

based on the fact that the PDF of underlying cosmological density fields is well described by the log-normal distribution (Kayo, Taruya, & Suto 2001). It is not clear whether the log-normal distribution can also describe the PDF of halo number densities which is more closely related to neighboring galaxy counts. Here we adopt the mock galaxy catalog used in Section 4 to check this log-normal assumption more directly.

We consider halo catalogs with masses of $M = 10^{13} h^{-1} M_{\odot}$ and $10^{14} h^{-1} M_{\odot}$. For each halo sample, we count the number of neighboring halos within the maximum transverse distance $r_{p,\max}$ and the redshift interval $\pm \Delta z = 0.02$, as in the case for our neighboring galaxy counts. We consider all halos with the masses higher than $10^{11} h^{-1} M_{\odot}$ which correspond roughly to the resolution limit of the Millennium Run simulation.

Figure A1 shows the PDFs of the number of neighboring halos around $M = 10^{13} h^{-1} M_{\odot}$ and $10^{14} h^{-1} M_{\odot}$ halos, for the maximum transverse separations of $r_{p,\max} = 1, 3,$ and $10 h^{-1} \text{Mpc}$. We find that the log-normal distribution generally fits very well. A possible exception is the case for small $r_{p,\max}$ and the halo mass of $M = 10^{14} h^{-1} M_{\odot}$ for which effects of halo exclusion and non-Gaussian error are most prominent, but even in this case the log-normal distribution provides a reasonably good approximation. Given the log-normal PDF of halo number counts, we expect neighboring galaxy counts also obey the long-normal distribution.